

# Formation of Water Chains on CaO(001): What Drives the 1D Growth?

Xunhua Zhao,<sup>†</sup> Xiang Shao,<sup>†,‡</sup> Yuichi Fujimori,<sup>†</sup> Saswata Bhattacharya,<sup>†</sup> Luca M. Ghiringhelli,<sup>†</sup> Hans-Joachim Freund,<sup>†</sup> Martin Sterrer,<sup>†,§</sup> Niklas Nilius,<sup>\*,†,||</sup> and Sergey V. Levchenko<sup>\*,†</sup>

<sup>†</sup>Fritz-Haber-Institute, Max-Planck-Gesellschaft, Faradayweg 4-6, 14195 Berlin, Germany

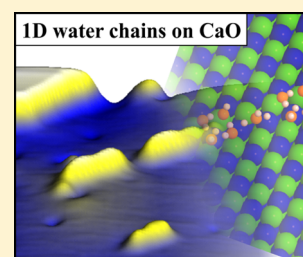
<sup>‡</sup>Department of Chemical Physics, University of Science & Technology of China, Hefei 230026, China

<sup>§</sup>Institute of Physics, University of Graz, Universitaetsplatz 5, 8010 Graz, Austria

<sup>||</sup>Institute of Physics, Carl-von-Ossietzky University, 26111 Oldenburg, Germany

## S Supporting Information

**ABSTRACT:** Formation of partly dissociated water chains is observed on CaO(001) films upon water exposure at 300 K. While morphology and orientation of the 1D assemblies are revealed from scanning tunneling microscopy, their atomic structure is identified with infrared absorption spectroscopy combined with density functional theory calculations. The latter exploit an ab initio genetic algorithm linked to atomistic thermodynamics to determine low-energy H<sub>2</sub>O configurations on the oxide surface. The development of 1D structures on the C<sub>4v</sub> symmetric CaO(001) is triggered by symmetry-broken water tetramers and a favorable balance between adsorbate–adsorbate versus adsorbate–surface interactions at the constraint of the CaO lattice parameter.



One-dimensional (1D) structures fascinate researchers in both physics and chemistry. Due to their basic topology, they are attractive model systems to explore quantization and transport phenomena of electrons and light<sup>1–3</sup> and serve as an ideal starting point to control molecular interactions.<sup>4</sup> Various mechanisms have been identified to promote formation of 1D assemblies. A fundamental requirement is a loss in symmetry that favors one growth direction against another. Linear growth can be induced on suitable templates, for example, stepped or patterned surfaces,<sup>5–7</sup> or by using uniaxial building blocks with active centers located at opposite sides.<sup>4,8</sup> Moreover, it may be triggered by a specific alignment of dipoles or charges along the growth direction.<sup>9</sup>

Water appears to be a good candidate for the formation of 1D structures as it possesses a strong dipole moment and is therefore inherently asymmetric. So far, 1D water assemblies were found on template surfaces exposing a linear texture,<sup>10</sup> for example, on Cu(110) and TiO<sub>2</sub>(110).<sup>11,12</sup> However, on most metallic or dielectric surfaces, water agglomerates into 2D networks as it interacts not only via dipole coupling but also via hydrogen bonding between the O and H species. The subtle interplay between the two schemes leads to the occurrence of “magic” water clusters, as identified with scanning tunneling microscopy (STM) and density functional theory (DFT).<sup>13,14</sup> The situation becomes even more complex if the molecules partly dissociate and the 2D network gets further stabilized by H<sub>2</sub>O–OH interactions and proton exchange between them.<sup>15</sup> Partly dissociated water layers have been found on many alkaline-earth oxides, for example, MgO, CaO, and SrO, by experiment<sup>16,17</sup> and theory.<sup>18–20</sup> In contrast, no 1D structures were identified on any of those systems so far. In this study, we

discuss the chain-like organization of partly dissociated water molecules on CaO(001), being a four-fold-symmetric surface without distinguished growth direction. According to DFT calculations, the 1D structures arise from an initial symmetry breaking, caused by a single proton located outside of an otherwise self-contained H<sub>2</sub>O tetramer complex.

The experiments were performed on 20 ML thick (001)-terminated CaO films,<sup>21</sup> exposing wide, atomically flat terraces delimited by a network of dislocation lines (Figure 1a). Small amounts of water (0.01–1 Langmuir) were dosed onto the freshly prepared films at 300 K. After exposure, protruding lines appeared in the STM that followed the CaO[110] direction, hence a Ca or O atomic row. Up to 0.15 L water coverage, the length of the ad-chains increased linearly from 1 to 15 nm (Figure 1b,c). At higher exposure, the initially isolated chains merged into an apparently disordered water adlayer (Figure 1d). The formation of 1D assemblies was found to depend critically on the adsorption conditions. Whereas low-temperature exposure (100 K) only led to amorphous surface configurations, the H<sub>2</sub>O sticking coefficient turned to zero at temperatures above 300 K, and the oxide remained clean.

The chemical nature of the ad-chains was explored with infrared reflection absorption spectroscopy (IRAS), performed on CaO(001) films exposed to 0.15 L D<sub>2</sub>O at 300 K (Figure 2). The spectra revealed two characteristic OD stretch vibrations at 2725 and 2600 cm<sup>–1</sup>. By comparison with previous IRAS data acquired on MgO-supported water structures,<sup>17</sup> they are

Received: February 2, 2015

Accepted: March 18, 2015

Published: March 18, 2015

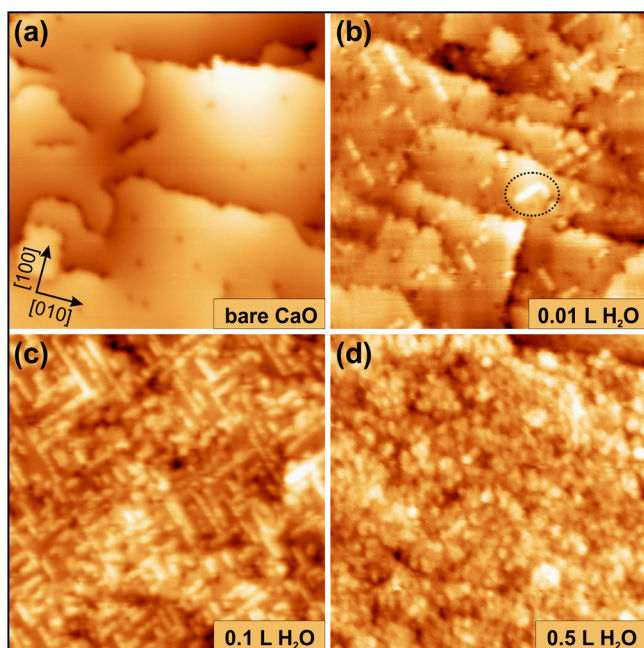


**Figure 1.** STM images of 20 ML CaO(001) (a) before and (b–d) after water exposure at 300 K ( $50 \times 50 \text{ nm}^2$ , 3.5 V, 25 pA). Water chains appear as bright lines running along the CaO[110] directions. The dashed circle denotes a rarely observed bent structure. Higher dosage results in amorphous adlayers and surface roughening (d).

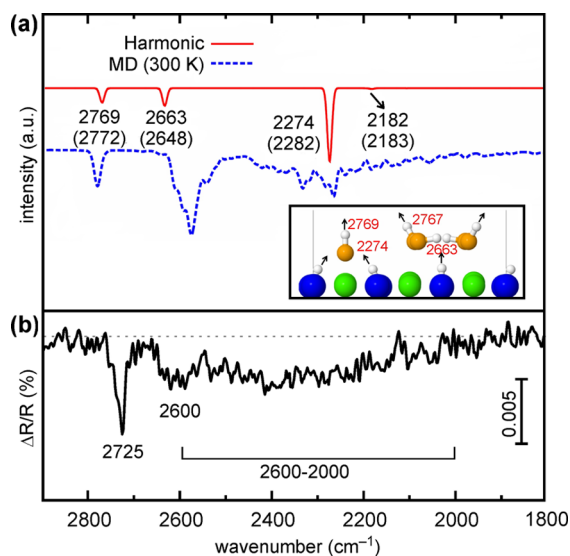


**Figure 2.** (a) Harmonic (red) and anharmonic (blue) vibrational spectra (300 K) of  $\text{D}_2\text{O}$  chains on CaO(001), calculated with PBE. HSE06 harmonic frequencies are shown in parentheses. The inset shows an assignment of the individual vibrational modes in the water ad-chains. (b) Experimental IR spectrum of 0.15 L  $\text{D}_2\text{O}$  dosed onto 20 ML CaO(001) at 300 K.

assigned to free  $\text{O}_{\text{f}}\text{D}$  ( $2725 \text{ cm}^{-1}$ ) and surface  $\text{O}_{\text{s}}\text{D}$  groups ( $2600 \text{ cm}^{-1}$ ). While the former constitutes the residual OD of a dissociated molecule, the latter contains an O ion of the oxide film. Besides these narrow maxima, a broad band is found between  $2600$  and  $2000 \text{ cm}^{-1}$  that, following the assignment on MgO(001), is attributed to molecular  $\text{D}_2\text{O}$ . Both spectral fingerprints indicate a coexistence of molecular and dissociated water in the 1D structures on CaO(001), a statement that will be corroborated by theory next.

To unravel the structure and thermodynamic stability of the water chains, we have performed DFT calculations with a hybrid exchange–correlation functional plus van der Waals (vdW) correction. In agreement with earlier studies,<sup>19,20</sup> dissociative adsorption is preferred over molecular binding for monomers and dimers (Figure 3a,b). The  $\text{O}_{\text{f}}\text{H}$  fragments thereby occupy Ca bridge sites at the surface, similar to the behavior found on MgO(001).<sup>22,23</sup> The lateral distance between the surface  $\text{O}_{\text{s}}\text{H}$  and the free  $\text{O}_{\text{f}}\text{H}$  of the monomer amounts to  $1.5 \text{ \AA}$ . In the dimer, the four hydroxyl species bind along a [110]-oriented oxygen row in the CaO surface. Partial dissociation occurs first in the water trimer that comprises one intact and two dissociated molecules in the center and at the ends, respectively (Figure 3c). Also, the tetramer is composed of two intact and two dissociated entities, located on the diagonal positions of a distorted square (Figure 3d). The square shape is governed by the surface Ca atoms that are  $3.4 \text{ \AA}$  apart ( $1/\sqrt{2}$  times the CaO lattice constant). Whereas one dissociated  $\text{O}_{\text{s}}\text{H}$  species sits inside of the square, the other one occupies an adjacent O position outside of the tetramer cluster. It is this extra hydroxyl that breaks the symmetry of the otherwise self-contained water aggregate and triggers the formation of linear chains. In fact, the fifth molecule binds to this extra  $\text{O}_{\text{s}}\text{H}$  in a dissociated configuration, creating a linker to the next tetramer cluster. Attachment of further molecules to the  $5\text{H}_2\text{O}$  cluster occurs in line with the linker, while orthogonal positions on the square are less preferred by  $0.06 \text{ eV}$ . A  $90^\circ$  bending of the chain is therefore unlikely, and the molecular assembly evolves straightly along a CaO[110] direction (Figure 3e,f). Also experimentally,  $90^\circ$  turns are rarely observed (Figure 1b, circle), and the majority of water chains are strictly linear.

At higher molecular packing, the 1D water structures transform into a 2D hydrogen-bonded network, similar to the one on MgO(001).<sup>17,18</sup> This scenario is depicted for 12 molecules per  $(3 \times 4)$  cell, that is, for a nominal coverage of 1 ML (Figure 3g). Also here, intact and dissociated entities form square-shaped building blocks; however, they homogeneously cover the entire surface as each Ca ion carries either a  $\text{H}_2\text{O}$  or  $\text{O}_{\text{f}}\text{H}$  unit. It is therefore the high surface coverage that triggers a breakdown of the 1D regime. For even higher loads (15 molecules per  $3 \times 4$  cell), both anionic and cationic surface sites get occupied with either intact molecules or  $\text{O}_{\text{f}}\text{H}$  groups, producing a dense hydrogen-bonded network (Figure 3h). Interestingly, such structures are largely stabilized by vdW forces and would desorb without this energetic contribution at experimental temperature and pressure conditions.

For the linear  $5\text{D}_2\text{O}/(3 \times 4)$  configuration shown in Figure 3e, harmonic and 300 K anharmonic vibrational spectra have been calculated and compared with the IRAS data of Figure 2. The main modes arise from the  $\text{O}_{\text{f}}\text{D}$  in tetramer and linker units that produce a quasi-degenerate band at  $\sim 2770 \text{ cm}^{-1}$ , as well as from the  $\text{O}_{\text{s}}\text{D}$  groups inside ( $\sim 2630 \text{ cm}^{-1}$ ) and outside of the tetramer ( $\sim 2300 \text{ cm}^{-1}$ ). The two intact molecules of the tetramer lie almost parallel to the surface and contribute little to the IR spectrum (small peak at  $2182 \text{ cm}^{-1}$ ). Finite temperature leads to a substantial broadening of the vibrational bands that mainly affects the region below  $2500 \text{ cm}^{-1}$ . The resulting band contains the symmetric and antisymmetric stretch modes of molecular water and a doublet structure due to anharmonically coupled symmetric and antisymmetric stretch combinations of the  $\text{O}_{\text{s}}\text{D}$  in the linker. The anharmonic calculation is in line with main features of the experimental spectrum, corroborating

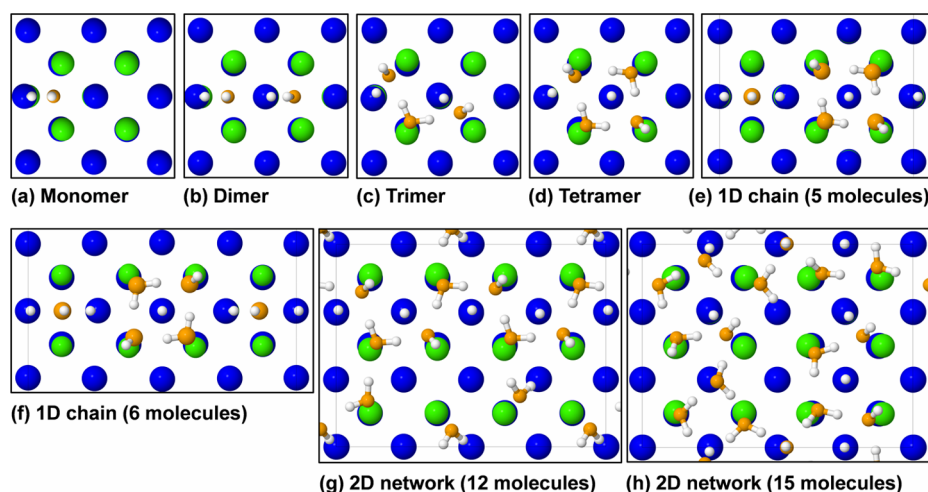


**Figure 3.** Energetically favorable adsorption structures for (a–f) 1–6, (g) 12, and (h) 15 water molecules on a (3 × 4) CaO(001) supercell. The O and Ca atoms of the film are depicted in blue and green, and the water O and H species are represented in orange and gray, respectively.

our conclusion that both intact and dissociated water species are present in the 1D chains. Only the doublet at  $2300\text{ cm}^{-1}$ , related to  $\text{O}_{\text{(s)}}\text{D}$  groups in the linker, is hardly resolved in the IRAS data, probably due to interference effects between coexisting water structures on the CaO surface.

The formation of 1D water structures on CaO(001) not only results from a certain growth preference at low coverage, hence is kinetically controlled, but represents a clear minimum in the binding energy per molecule (Figure 4a). On the basis of

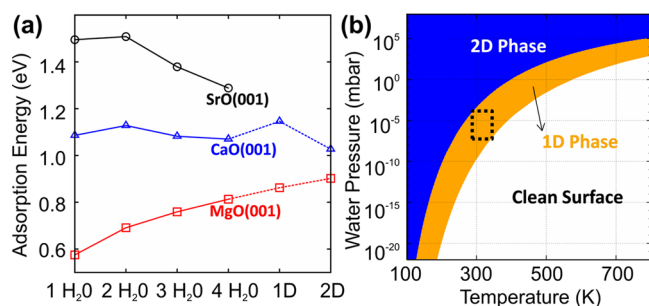


**Figure 4.** (a) HSE06+vdW adsorption energy per water molecule on CaO(001), MgO(001), and SrO(001), including zero-point energy contributions. (b) Phase diagram of adsorbed water on CaO(001), as calculated with HSE06+vdW including the vibrational free energy. The dashed square denotes the experimental conditions.

HSE06+vdW calculations, an isolated  $\text{H}_2\text{O}$  binds with 1.09 eV to the surface. This value increases to 1.12 eV for the dimer, reflecting the stabilizing effect of intermolecular coupling. When more molecules are added to the aggregate, the binding energy decreases first but reaches another maximum of 1.15 eV for the ad-chains. As binding becomes weaker in dense molecular assemblies, the 1D water chains are indeed energetically preferred among all structures considered here. This trend becomes manifest also in the surface phase diagram (Figure 4b). In a narrow ( $T, p$ ) region, 1D structures are thermodynamically preferred over the 2D network, proving that not only kinetic but also thermodynamic aspects are responsible for the linear arrangement of water on CaO(001). The relatively narrow stability range of the chain structures agrees well with the observation of amorphous  $\text{H}_2\text{O}$

adlayers at slightly lower temperature or larger exposure times in the experiment (Figure 1d).

Surprisingly, 1D water chains are thermodynamically unfavorable on isostructural MgO(001) and SrO(001) surfaces. Whereas on MgO linear ad-structures are metastable and evolve spontaneously into a 2D network, complete dissociation and formation of random OH configurations is revealed on SrO(001). Our calculations indicated that the 1D structures on CaO(001) are stabilized by a subtle balance between intermolecular and molecule–surface interactions. In fact, the CaO lattice is slightly too large to enable the formation of a hydrogen-bonded network, and the water structures therefore collapse into a 1D configuration at low coverage. Similar 1D assemblies become stable also on MgO(001) when its lattice parameter is artificially increased to reduce the effect of intermolecular coupling. In contrast on SrO(001), the water residuals are always too far away to form uniaxial hydrogen-bonded arrangements.

In conclusion, formation of 1D molecular assemblies is observed upon water exposure onto a four-fold-symmetric CaO(001) surface. The required symmetry breaking occurs at the level of tetramer clusters, consisting of self-containing  $[\text{H}_2\text{O}-\text{O}_{\text{(f)}}\text{H}]$  square structures with one  $\text{O}_{\text{(s)}}\text{H}$  inside and another one outside of the unit. This outer hydroxyl serves as a docking site for subsequent water molecules, resulting in the growth of water chains along the CaO[110] direction. The development of 1D water structures is unique to CaO(001) and enabled by the favorable binding distance of the water entities on the surface.

## ■ EXPERIMENTAL AND THEORETICAL METHODS

CaO films of 20 ML thickness were prepared by reactive Ca deposition onto a sputtered and annealed Mo(001) surface in  $5 \times 10^{-7}$  mbar  $\text{O}_2$  at 300 K.<sup>21</sup> Their crystallization was achieved by vacuum annealing to 1000 K, resulting in well-ordered (001)-terminated rocksalt-type films as deduced from low-energy electron diffraction. STM measurements revealed a homogeneous surface morphology, characterized by atomically flat terraces delimited by a dislocation network (Figure 1a). Small amounts of water (0.01 to 1 Langmuir) were dosed via a leak valve onto the freshly prepared samples at 300 K. The chemical nature of the water assemblies was probed with IRAS using a Bruker IFS 66v FTIR spectrometer combined with a



MCT detector. The spectrum of a clean, freshly prepared CaO(001) film was used for background correction. The resolution was set to  $4\text{ cm}^{-1}$ , and 1000 scans were accumulated to obtain a reasonable signal-to-noise ratio.

Structural properties of the water chains were elucidated by DFT calculations performed with a hybrid exchange–correlation functional (HSE06)<sup>24</sup> plus vdW correction,<sup>25</sup> as implemented in the all-electron code FHI-aims.<sup>26</sup> The vdW correction per molecule was determined to  $\sim 0.15\text{ eV}$ , making it relevant at the experimental temperature. The different 1D and 2D configurations were obtained with an ab initio genetic algorithm (GA),<sup>17,27</sup> starting from random water assemblies on the surface. During the GA search, the PBE functional was used, while the resulting structures were relaxed on the HSE06 level. This postrelaxation scheme was shown to preserve structural elements of the low-energy isomers but cannot guarantee that all (meta)stable isomers were found in a given energy window. To evaluate the relative stability of the water assemblies at realistic conditions, the surface free energy was calculated by ab initio atomistic thermodynamics.<sup>28</sup> Hereby, also nonstoichiometric ad-structures were considered but found to be unstable at realistic temperatures and pressures. The configurational entropy was disregarded; however, rough estimates on the basis of Boltzmann's entropy formula indicated that the 1D structures prevail at experimental conditions. Vibrational spectra of water adlayers were calculated in the harmonic approximation on the PBE and HSE06 level. In addition, finite-temperature anharmonic spectra were obtained from the dipole–dipole autocorrelation function calculated with ab initio molecular dynamics at the PBE level. No scaling factors were applied, and our analysis was restricted to the  $z$ -component of the autocorrelation function as only dipole moments perpendicular to the surface have been observed experimentally. More details on computational methods and their validation are given in the Supporting Information.

## ■ ASSOCIATED CONTENT

### ■ Supporting Information

Computational details, including DFT calculations, the calculated IR spectrum, and additional information on the adsorbed water structures. This material is available free of charge via the Internet at <http://pubs.acs.org>.

## ■ AUTHOR INFORMATION

### Corresponding Authors

\*E-mail: [niklas.nilius@uni-oldenburg.de](mailto:niklas.nilius@uni-oldenburg.de) (N.N.).

\*E-mail: [levchenko@fhi-erlin.mpg.de](mailto:levchenko@fhi-erlin.mpg.de) (S.V.L.).

### Notes

The authors declare no competing financial interest.

## ■ ACKNOWLEDGMENTS

We thank Matthias Scheffler for insightful discussions. This work was supported by the DFG Excellence Cluster "UNICAT", and the COST Action CM1104. M.S. acknowledges support by the European Union through the ERC Starting Grant Agreement 280070. Y.F. is grateful to DAAD and Co. Ltd. TAKATA.

## ■ REFERENCES

(1) Nilius, N.; Wallis, T. M.; Ho, W. Development of one-dimensional band structure in artificial gold chains. *Science* **2002**, *297*, 1853–1856.

(2) Nagao, T.; Yaginuma, S.; Inaoka, T.; Sakurai, T. One-dimensional plasmon in an atomic-scale metal wire. *Phys. Rev. Lett.* **2006**, *97*, 116802.

(3) Blumenstein, C.; Schäfer, J.; Mietke, S.; Meyer, S.; Dollinger, A.; Lochner, M.; Cui, X. Y.; Patthey, L.; Matzdorf, R.; Claessen, R. Atomically controlled quantum chains hosting a Tomonaga–Luttinger liquid. *Nat. Phys.* **2011**, *7*, 776–780.

(4) Barth, J. V.; Costantini, G.; Kern, K. Engineering atomic and molecular nanostructures at surfaces. *Nature* **2005**, *437*, 671–679.

(5) Gambardella, P.; Dallmeyer, A.; Maiti, K.; Malagoli, M. C.; Rusponi, S.; Ohresser, P.; Eberhardt, W.; Carbone, C.; Kern, K. Oscillatory magnetic anisotropy in one-dimensional atomic wires. *Phys. Rev. Lett.* **2004**, *93*, 077203.

(6) Gurlu, O.; Adam, O. A.; Zandvliet, H. J.; Poelsema, B. Self-organized, one-dimensional Pt nanowires on Ge (001). *Appl. Phys. Lett.* **2003**, *83*, 4610–4612.

(7) Donadio, D.; Ghiringhelli, L. M.; Delle Site, L. Autocatalytic and cooperatively stabilized dissociation of water on a stepped platinum surface. *J. Am. Chem. Soc.* **2012**, *134*, 19217–19222.

(8) Li, Q.; Owens, J. R.; Han, C.; Sumpter, B. G.; Lu, W.; Bernholc, J.; Meunier, V.; Maksymovych, P.; Fuentes-Cabrera, M.; Pan, M. Self-organized and Cu-coordinated surface linear polymerization. *Sci. Rep.* **2013**, *3*, 2102.

(9) Simic-Milosevic, V.; Heyde, M.; Lin, X.; König, T.; Rust, H.-P.; Sterrer, M.; Risse, T.; Nilius, N.; Freund, H.-J.; Giordano, L.; Pacchioni, G. Charge-induced formation of linear Au clusters on thin MgO films: Scanning tunneling microscopy and density-functional theory study. *Phys. Rev. B* **2008**, *78*, 235429.

(10) Carrasco, J.; Hodgson, A.; Michaelides, A. A molecular perspective of water at metal interfaces. *Nat. Mater.* **2012**, *11*, 667–674.

(11) Carrasco, J.; Michaelides, A.; Forster, M.; Haq, S.; Raval, R.; Hodgson, A. A one-dimensional ice structure built from pentagons. *Nat. Mater.* **2009**, *8*, 427–431.

(12) Lee, J.; Sorescu, D. C.; Deng, X.; Jordan, K. D. Water chain formation on  $\text{TiO}_2(110)$ . *J. Phys. Chem. Lett.* **2012**, *4*, 53–57.

(13) Michaelides, A.; Morgenstern, K. Ice nanoclusters at hydrophobic metal surfaces. *Nat. Mater.* **2007**, *6*, 597–601.

(14) Shin, J. W.; Hammer, N. I.; Diken, E. G.; Johnson, M. A.; Walters, R. S.; Jaeger, T. D.; Duncan, M. A.; Christie, R. A.; Jordan, K. D. Infrared signature of structures associated with the  $\text{H}^+(\text{H}_2\text{O})_n$  ( $n = 6$  to  $27$ ) clusters. *Science* **2004**, *304*, 1137–1140.

(15) Rybkin, V. V.; Simakov, A. O.; Bakken, V.; Reine, S.; Kjærgaard, T.; Helgaker, T.; Uggerud, E. Insights into the dynamics of evaporation and proton migration in protonated water clusters from large-scale Born–Oppenheimer direct dynamics. *J. Comput. Chem.* **2013**, *34*, 533–544.

(16) Kim, Y. D.; Stultz, J.; Goodman, D. W. Dissociation of water on  $\text{MgO}(100)$ . *J. Phys. Chem. B* **2002**, *106*, 1515–1517.

(17) Włodarczyk, R.; Sierka, M.; Kwapien, K.; Sauer, J.; Carrasco, E.; Aumer, A.; Gomes, J. F.; Sterrer, M.; Freund, H. J. Structures of the ordered water monolayer on  $\text{MgO}(001)$ . *J. Phys. Chem. C* **2011**, *115*, 6764–6774.

(18) Giordano, L.; Goniakowski, J.; Suzanne, J. Partial dissociation of water molecules in the  $(3 \times 2)$  water monolayer deposited on the  $\text{MgO}(100)$  surface. *Phys. Rev. Lett.* **1998**, *81*, 1271.

(19) Hu, X. L.; Carrasco, J.; Klimeš, J.; Michaelides, A. Trends in water monomer adsorption and dissociation on flat insulating surfaces. *Phys. Chem. Chem. Phys.* **2011**, *13*, 12447–12453.

(20) Carrasco, J.; Illas, F.; Lopez, N. Dynamic ion pairs in the adsorption of isolated water molecules on the alkaline-earth oxide (001) surfaces. *Phys. Rev. Lett.* **2008**, *100*, 016101.

(21) Shao, X.; Myrach, P.; Nilius, N.; Freund, H. J. Growth and morphology of calcium-oxide films grown on  $\text{Mo}(001)$ . *J. Phys. Chem. C* **2011**, *115*, 8784–8789.

(22) Honkala, K.; Hellman, A.; Grönbeck, H. Water dissociation on  $\text{MgO}/\text{Ag}(100)$ : Support induced stabilization or electron pairing. *J. Phys. Chem. C* **2010**, *114*, 7070–7075.

- (23) Carrasco, E.; Brown, M. A.; Sterrer, M.; Freund, H.-J.; Kwapien, K.; Sierka, M.; Sauer, J. Thickness-dependent hydroxylation of MgO(001) thin films. *J. Phys. Chem. C* **2010**, *114*, 18207–18214.
- (24) Heyd, J.; Scuseria, G. E.; Ernzerhof, M. Hybrid functionals based on a screened Coulomb potential. *J. Chem. Phys.* **2006**, *124*, 219906.
- (25) Tkatchenko, A.; DiStasio, R. A., Jr.; Car, R.; Scheffler, M. Accurate and efficient method for many-body van der Waals interactions. *Phys. Rev. Lett.* **2012**, *108*, 236402.
- (26) Blum, V.; Gehrke, R.; Hanke, F.; Havu, P.; Havu, V.; Ren, X.; Reuter, K.; Scheffler, M. Ab initio molecular simulations with numeric atom-centered orbitals. *Comput. Phys. Commun.* **2009**, *180*, 2175–2196.
- (27) Chuang, F. C.; Ciobanu, C. V.; Shenoy, V. B.; Wang, C. Z.; Ho, K. M. Finding the reconstructions of semiconductor surfaces via a genetic algorithm. *Surf. Sci.* **2004**, *573*, L375–L381.
- (28) Reuter, K.; Scheffler, M. Composition and structure of the RuO<sub>2</sub>(110) surface in an O<sub>2</sub> and CO environment: Implications for the catalytic formation of CO<sub>2</sub>. *Phys. Rev. B* **2001**, *65*, 035406.